LAWRENCE
LIVERMORE
NATIONAL
LABORATORY

UCRL-PROC-217797

The Development of a Detailed Chemical Kinetic Mechanism for Diisobutylene and Comparison to Shock Tube Ignition Times

Wayne K. Metcalfe, William J. Pitz, Henry J. Curran, John M. Simmie, Charles K. Westbrook

December 19, 2005

31st International Symposium on Combustion
Heidelberg, Germany
August 6, 2006 through August 6, 2006

The Development of a Detailed Chemical Kinetic Mechanism for Diisobutylene and Comparison to Shock Tube Ignition Times

Wayne K. Metcalfe[a], William J. Pitz[b] Henry J. Curran[a], John M. Simmie[a],

and Charles K. Westbrook[b]

[a]National University of Ireland, Galway.

[b]Lawrence Livermore National Laboratory, Livermore, CA 94551

Wayne Metcalfe,
Chemistry Department,
National University of Ireland, Galway,
Ireland.
wayne.metcalfe@nuigalway.ie
Reaction Kinetics

Total Length (M1)	5050
Total length including abstract	5225

Individual lengths

Main text	2874
References (M1)	385
Table 1 + caption (M1)	133
Figure 1 +caption (M1)	147
Figure 2 +caption (M1)	188
Figure 3 +caption (M1)	201
Figure 4 +caption (M1)	185
Figure 5 +caption (M1)	146
Figure 6 +caption (M1)	177
Figure 7 +caption (M1)	183
Figure 8 +caption (M1)	183
Figure 9 +caption (M1)	189
figure 10 +caption(M1)	59

Abstract

Shock tube experiments and chemical kinetic modeling were carried out on 2,4,4-trimethyl-1-pentene and 2,4,4-trimethyl-2-pentene, the two isomers of diisobutylene, a compound intended for use as an alkene component in a surrogate diesel fuel. Ignition delay times were obtained behind reflected shock waves at 1 and 4 atm, and between temperatures of 1200 and 1550 K. Equivalence ratios ranging from 1.0 to 0.25 were examined for the 1-pentene isomer. A comparative study was carried out on the 2-pentene isomer and on the blend of the two isomers. It was found that the 2-pentene isomer ignited significantly faster under shock tube conditions than the 1-pentene isomer and that the ignition delay times for the blend were directly dependant on the proportions of each isomer. These characteristics were successfully predicted using a detailed chemical kinetic mechanism. It was found that reactions involving isobutene were important in the decomposition of the 1-pentene isomer. The 2-pentene isomer reacted through a much different pathway involving resonantly stabilized radicals, highlighting the effect on the chemistry of a slight change in molecular structure.

Keywords: Ignition, diisobutylene, shock tube, chemical kinetics

1. **Introduction**

There is much demand for chemical kinetic models to represent practical fuels such as gasoline, diesel and aviation fuel. These blended fuels may contain hundreds of components whose identity and amounts are often unknown. A chemical kinetic mechanism that would represent the oxidation of all these species with accompanying chemical reactions is intractable with current computational capabilities, chemical knowledge and manpower resources. The use of surrogate fuels is an approach to make the development of chemical kinetic mechanisms for practical fuels tractable. A surrogate fuel consists of a small number of components that can be used to represent the practical fuel and still predict characteristics of the real fuel. Desired fuel characteristics may include ignition behavior, burning velocity, viscosity, vaporization, and emissions (carbon monoxide, hydrocarbons, soot and nitrogen oxides).

Gasoline consists of many different classes of hydrocarbons including straight and branched alkanes, cycloalkanes, alkenes, cycloalkenes, and aromatics. One approach to surrogate fuels is to include one or more

components from each class of hydrocarbon in gasoline so that the unique molecular structure of each class is represented. This approach may lead to reliable predictions of many of the combustion properties of the practical fuel. In order to obtain a fuel surrogate mechanism, detailed chemical kinetic mechanisms must be developed for each component in the mix compound.

In this study, a detailed chemical kinetic mechanism is developed for diisobutylene, which is intended to represent the hydrocarbon class of alkenes in practical fuels. Diisobutylene is not a pure compound but is a mixture of two conjugate olefins of iso-octane: 2,4,4-trimethyl-1- (and -2-) pentene. Diisobutylene has a similar molecular structure to iso-octane, so that its kinetics offers an insight into the effect of including a double bond in the carbon skeletal structure of iso-octane.

There are few previous studies on diisobutylene. Kaiser *et al.* [1] examined the exhaust emissions from a production spark ignition engine with neat diisobutylene and a mixture of it with gasoline. They found that the exhaust emissions of diisobutylene are similar to that of iso-octane. However a significant increase in the amount of 2-methyl-1,3-butadiene was observed in the exhaust of the engine relative to iso-octane. They also found appreciable amounts of propene in the exhaust, but could not explain the source of this product in terms of C-C bond beta scission of alkyl radicals. More recently Risberg *et al.* [2] studied a number of fuel blends to evaluate their autoignition quality for use in a homogeneous charge compression ignition engine, using diisobutylene to represent olefins in one of their test fuels.

In this study, experiments on the shock tube ignition of both isomers of diisobutylene will be described. Then, the development of a detailed chemical kinetic mechanism for the two isomers of diisobutylene will be discussed. Finally, the mechanism will be applied to the shock tube ignition of diisobutylene.

2. **Experimental**

All shock tube measurements presented in this paper were obtained in a helium-driven shock tube built and characterized at the National University of Ireland, Galway [3]. The experimental apparatus consists of a shock tube, gas handling facility, and light emission diagnostic.

2.1 Apparatus

The stainless steel shock tube consists of a 53 cm long, 52 cm outer diameter driver section, terminated at one end with a 10 cm long, 10.24 cm internal diameter tube, which is separated from the 6 m long, 10.24 cm internal diameter test section by a diaphragm. Shock waves were generated not by allowing the polycarbonate diaphragm (Makrofol DE, Coloprint GmbH) to burst under pressure alone, but with the aid of a cross-shaped cutter to ensure uniform petalling of the diaphragm. A series of four pressure transducers (PCB 113A21) mounted flush with the internal wall, and located at precise distances from the end-wall were used to measure the incident shock velocity using three universal time counters (Fluke/Phillips PM6666). In order to allow for shock attenuation, the shock velocity at the end-wall was calculated by linearly extrapolating the incident shock velocity to the end-wall.

The emission of CH^* behind the reflected shock wave was monitored using an end-on detection diagnostic [4], consisting of a photodiode array detector (Thorlabs Inc., model PDA55), located directly behind a 431 nm narrow band-pass filter with a spectral bandwidth of 10 nm. Both the filter and the PDA are aligned behind a 6 mm outer diameter fused silica window embedded in the end-wall. Reflected shock conditions were calculated from shock velocities using the one-dimensional shock relations [5] and the application GASEQ [6]. The thermochemistry for diisobutylene was calculated using THERM [7].

2.2 *Mixture Preparation*

Test mixtures were prepared in a 35 L stainless steel tank using standard manometric methods. Gases were obtained from BOC Ireland Ltd.: Argon Zero Grade 99.998%, and Oxygen Research Grade 99.985%. All gases were used without further purification. The diisobutylene (99% pure) was obtained from Aldrich Chemical Co. Ltd. To minimize the presence of atmospheric air in the sample the liquid diisobutylene was subjected to several freeze-pump-thaw degassing cycles before being used. The liquid diisobutylene was incorporated into the mixing vessel by vaporization of the fuel into the evacuated mixing tank. Both fuel and oxygen partial pressures were measured using a 100 Torr Baratron gauge to an accuracy of 0.01 Torr. For reactant gas pressures above 100 Torr, a Wallace and Tiernan 800 Torr absolute pressure gauge was used. Test gas mixtures were normally made up to a final pressure of 800 Torr. To ensure homogeneity, the mixtures were allowed to stand for 24 hours or mixed for two hours using a magnetic stirring bar. (Both methods gave consistent results, indicating adequate mixing was obtained using either method) From the resulting mix, initial pressures, (P_1), varying from 20 to 100 Torr were used during these experiments.

Prior to an experiment both the driver and driven sections of the shock tube were evacuated independently. The driver section was evacuated to 10^{-3} Torr using a rotary oil pump, while the driven section was firstly pumped to 10^{-2} Torr using a rotary oil pump, and the final pressure of 10^{-6} Torr was achieved using a diffusion pump. The range of experimental data generated for 2,4,4-trimethyl-1-pentene is provided in Table 1.

2.3 Ignition Delays

All ignition delay times, τ, for the current study were measured behind the reflected shock, with τ defined as the time interval from shock arrival at the end-wall, as indicated by an in-situ pressure transducer (Kistler 601H), to the maximum in the rate of change of emission of light from CH^* at 431 nm with respect to time. This definition is taken from that of Gutman et al. [4] where a similar end-wall diagnostic was used to measure the emission of light from the reaction $CO + O \rightarrow CO_2 + h\nu$.

3. Chemical Kinetic Model

The chemical kinetic model for diisobutylene was constructed based on the iso-octane mechanism of Curran et al. [8]. (The current version of the iso-octane mechanism is available at the LLNL mechanism website [9].) Due to the importance of the isobutene submechanism to the chemistry of the 1-pentene isomer (discussed below), the C_4 portion of the mechanism has been amended taking the work of Curran [10] into account. A full listing of this mechanism is available from the authors. Species and reactions were added to the iso-octane mechanism to treat the oxidation of both isomers of diisobutylene (DIB). (DIB will be used as shorthand below to refer to both isomers.) The diisobutylene isomers were already present in the iso-octane mechanism, so that some reactions and species were already included. There are several different types of reactions that were added. Examples of these types of reactions and the source of their rate constants are discussed below.

3.1 *Initiation reactions*

Molecular elimination reactions for DIB were added using the rate constants of Tsang [11]. These reactions are also called retroene reactions [12]. A retroene reaction (Fig. 1) is only possible from the 1-pentene

isomer (jc8h16). No six-membered elimination is possible for the 2-pentene isomer (ic8h16). The retroene reaction was not found to play a role in the shock tube ignition of DIB.

Both C-C and C-H bond breaking reactions were included for the parent fuel. The high-pressure rate constants were specified by their reverse rate constants with the forward decomposition rate constants being computed from microscopic reversibility. The C-H bond breaking reaction rates are slow, but were included because they were important in the reverse direction under shock tube conditions. The pressure and temperature dependence of the fuel decomposition reaction rate constants were computed using Quantum RRK analysis to obtain k(E) and master equation analysis to evaluate pressure fall-off [13]. For the master equation analysis, an exponential-down energy-transfer model was used, with a collisional step-size down (ΔE_{down}) of 350 cm^{-1} for an Ar collider. The addition of these factors decreased the ignition delays for the 1-pentene isomer slightly. Reaction of DIB with O_2 was also included, but it is not important under shock tube conditions. Under shock tube conditions, the decomposition of the 1-pentene isomer was much faster than the 2-pentene isomer of C_8H_{16}. The same rate constant for C-C bond breakage was assumed in the reverse direction for both isomers by analogy with the allyl + methyl radical combination reaction. However, in the forward decomposition direction, the pre-exponential factor computed from microscopic reversibility for the 1-pentene-isomer decomposition was much faster than the 2-pentene isomer. Shock tube ignition delay times are usually dependant on initiation reactions, but for the 1-pentene isomer the decomposition is so fast that it is not the rate determining step, with the ignition delay instead being sensitive to the decomposition of isobutene.

3.2 *Abstraction reactions*

Abstraction of H atoms from both alkylic and allylic C-H bonds in DIB was included in the mechanism. The abstraction from vinylic C-H bonds was neglected because the rate constants are much lower than that of allylic or alkyl C-H [12]. Abstraction by OH, H, CH_3, HO_2, CH_3O_2, CH_3O, C_2H_5, and C_2H_3 radicals were considered. For OH, H, CH_3 + DIB, the rate constant parameters for the abstraction of primary alkyl C-H were taken from Curran et al. [8]. The rate constants for the abstraction of primary and secondary allylic C-H bonds were taken from Heyberger et al. [14]. For HO_2 + DIB, rate constants were taken from Scott and Walker [15] for allylic and alkyl of C-H bonds. The rate constants for CH_3O_2 + DIB were assumed to be the same as HO_2 + DIB. The rate constants for CH_3O and C_2H_3 + DIB for the abstraction of allylic C-H are not available in the literature and were estimated.

3.3 *Decomposition of DIB radicals (C_8H_{15})*

The rate constants for the decomposition of DIB radicals were specified in the reverse exothermic direction. In this direction, the reaction is the addition of a radical to a double bond. The rate constants were taken from Curran [16].

3.4 *CH* submechanism*

A CH mechanism was included from Hall and Peterson [17]. Results form the mechanism showed that the reaction of $C_2H + O_2 = CO_2 + CH^*$ is the most important reaction in the formation of CH*. However, as experimental delays are defined by the time of maximum rate of change of CH* emission, we have found that the time of maximum product of $[C_2H] * [O]$ coincides best with the simulated time of maximum rate of change of CH* concentration and thus we have used this criterion in defining our ignition delay times

3.5 *Numerical model*

The simulations were carried out with CHEMKIN 3, using the Aurora code assuming constant pressure.

4. Results and Discussion

First we will discuss the results for 2,4,4-trimethyl-1-pentene. The experimental and computational results show how the ignition delay times are influenced by fuel concentration, oxygen concentration, and pressure. The influence of fuel concentration is seen in Fig. 2 where the ignition delay times increase with increasing fuel concentration. The reason for this behavior is that the fuel reacts with H atoms that would otherwise react with oxygen and provide chain branching through $H + O_2 = OH + O$. The effect of fuel concentration on ignition delay diminishes as the temperature is lowered (Fig. 2) until the effect is reversed for most hydrocarbon fuels at low temperatures [18]. Qualitatively, the trends with fuel concentration are similar in both the experimental and modeling results. The mechanism predicts ignition delay times that are in good agreement with those measured

experimentally. The magnitude of the decrease in ignition delay time with a decrease in fuel concentration (from 0.75% to 0.375%) is well reproduced by the model

At low temperatures, some strange behaviour is seen experimentally, as the data seems to curve over around 1350 K. This is not reproduced by the model. At this temperature the delays are quite long (> 1500 μs) thus testing the boundaries of the shock tube's reliability. After this length of time, the complex shockwave - contact surface / rarefraction wave interactions may be having unpredictable effects on the conditions inside the tube leading to unusual results.

The influence of oxygen concentration is seen in Fig. 3. The ignition delay time decreases as the oxygen concentration increases from 9% (squares) to 18% (circles). This behavior is commonly seen for hydrocarbons where ignition delay time has a negative exponent for its dependence on oxygen concentration [19], [20]. The effect of fuel concentration is also seen in Fig. 2. The fuel concentration is decreased from the data series shown as circles (0.75% fuel) to that shown as triangles (0.375% fuel). Again, this behavior is similar to other hydrocarbons, which show a slight positive exponent for the dependence of ignition delay time on fuel concentration. Fig. 3 shows that the effect of a factor of two change in oxygen concentration has a much more pronounced effect on ignition delay times than a factor of two change in fuel concentration. The model shows approximately correct dependence on oxygen concentration but predicts about a factor of two greater dependence on the fuel concentration than observed in the experiment.

The influence of pressure is seen in Fig. 4 where increasing pressure decreases the ignition delay time. The relative shift toward decreased ignition delay times with increasing pressure is well reproduced by the model. The predicted ignition delay times are in good agreement for the 1.0 atm data and about 25% too fast for the 4.0 atm case.

Finally, the effect of fuel composition is considered, examining both isomers and their mixtures (Fig. 5). The experiments show that 2,4,4-trimethyl-2-pentene (triangles) is considerably faster to ignite than 2,4,4-trimethyl-1-pentene (squares). In addition, the mixture that contains three parts 2,4,4-trimethyl-1-pentene to one part 2,4,4-trimethyl-2-pentene is intermediate to the pure components. Ignition delay times appear to be directly proportional to the quantity of each isomer present.

The comparative trends in the model results as the fuel is changed from 2,4,4-trimethyl-1-pentene to 2,4,4-trimethyl-2-pentene and to the mixture are quite similar to the experiment results (Fig. 5). The predicted delays for 2,4,4-trimethyl-2-pentene are approximately 40% too slow (Fig 6), but the prediction for the mixture is in excellent agreement with experiment.

4.1: *Sensitivity analysis*

A sensitivity analysis was carried out for both isomers at temperatures of 1242 and 1444 K. This was done by identifying the important reactions and increasing their rates by a factor of two and seeing the effect on the calculated ignition delay time (Figs. 7 and 8).

Figure 7 shows the dependence of ignition delay time of 2,4,4-trimethyl-1-pentene (jc8h16) on the chemistry of isobutene (ic4h8). The main decomposition pathway of jc8h16 is the formation of tc4h9 + ic4h7, with tc4h9 in turn producing isobutene. Ignition delay is far more sensitive to the decomposition of isobutene than to the decomposition of the fuel itself.

The primary decomposition pathway for 2,4,4-trimethyl-2-pentene (ic8h16) is shown in Fig. 9. It decomposes to a resonantly stabilized radical of 2,4-dimethyl-2-pentene (yc7h13-y2). Fig. 8 shows the sensitivity of ignition delay to this reaction and to the other reactions involved in this pathway. There is also sensitivity to the abstraction reactions producing the radicals jc8h15-b and ic8h15-a (Fig. 10). These both form 2,4-dimethyl-1,3-pentadiene (dmpd13), which is an intermediate in the decomposition shown in Fig. 9.

5. Conclusions

Ignition delay times for 2,4,4-trimethyl-1-pentene have been measured behind reflected shock waves at 4 atm and at equivalence ratios of 0.25, 0.5, and 1.0. Experiments performed at 1.0 and 4.0 atm with an equivalence ratio of 1.0 show the influence of pressure. In addition, the reactivity of pure 2,4,4-trimethyl-1-pentene, 2,4,4-trimethyl-2-pentene, and a 0.75 2,4,4-trimethyl-1-pentene / 0.25 2,4,4-trimethyl-2-pentene mixture was examined. It was found that of the two isomers, 2,4,4-trimethyl-2-pentene is significantly faster to ignite throughout the temperature range (1200—1550 K) of this study. The chemical kinetic mechanism developed to interpret these experiments reproduces these effects.

Acknowledgments

The work at Lawrence Livermore National Laboratory was supported by the U.S. Department of Energy, Office of Freedom CAR and Vehicle Technologies and under the auspices of the U.S. Department of Energy by

University of California, Lawrence Livermore National Laboratory under contract No. W-7405-Eng-48. The authors thank program managers Stephen Goguen and Gurpreet Singh for their support of this work. The work at the National University of Ireland, Galway was supported by the Environmental Protection Agency under the Doctoral Fellowship Scheme.

References

[1]. Kaiser, E. W., Slegl, W., Cotton, D. F. and Anderson, R. W., *Environ. Sci, Technol.* 27:1440-1447 (1993).

[2]. Risberg, P., Kalghatgi, G. and Angstrom, H.-E., *Auto-ignition Quality of Gasoline-Like Fuels in HCCI Engines*, Society of Automotive Engineers, SAE Paper 2003-01-3215, (2003).

[3]. Smith, J. M., Ph. D., PhD Thesis, National University of Ireland, Galway, 2004.

[4]. Gutman, D., Hardwidge, E. A., Dougherty, F. A. and Lutz, R. W., *J. Chem. Phys.* 47:4400-4407 (1967).

[5]. Gaydon, A. G. and Hurle, I. R., *The Shock Tube in High-Temperature Chemical Physics*, Chapman and Hall, London, (1963).

[6]. Morley, C. *GASEQ, http://www.c.morley.ukgateway.net/gseqrite.html*, 2005.

[7]. E. R. Ritter and J. W. Bozzelli, "THERM: Thermodynamic Property Estimation for Gas Phase Radicals and Molecules," *Int. J. Chem. Kinet.*, **23**, 767-778 (1991).

[8]. Curran, H. J., Gaffuri, P., Pitz, W. J. and Westbrook, C. K., *Combust. Flame* 129:253-280 (2002).

[9]. Pitz, W. J., Westbrook, C. K. and Curran, H. J. *LLNL Chemical Kinetic Mechanisms*, 2004.

[10] Curran, Ph.D Thesis, National University of Ireland, Galway, 1994.

[11]. Tsang, W., *Int. J. Chem. Kinet.* 10:1119-1138 (1978).

[12]. Richard, C., Scacchi, G. and Back, M. H., *Int. J. Chem. Kinet.* 10:307-324 (1978).

[13]. Sheng, C. Y. and Bozzelli, J. W., *Journal of American Chemical Society A* 106:7276-7293 (2002).

[14]. Heyberger, B., Belmekki, N., Conraud, V., Glaude, P.-A., Fournet, R. and Battin-Leclerc, F., *Int. J. Chem. Kinet.* 34(12):666-677 (2002).

[15]. Scott, M. and Walker, R. W., *Combust. Flame* 129(4):365-377 (2002).

[16]. Curran, H. J., *Int. J. Chem. Kinet.*, accepted (2005).

[17]. Hall, Joel M. and Rickard, Matthew J.A., *Combustion Science and Technology, submitted 2004.*

[18]. Ciezki, H. K. and Admeit, G., *Combust. Flame* 93:421-433 (1993).

[19]. Burcat, A., Scheller, K. and Lifshitz, A., *Combust. Flame* 16:29-33 (1971).

[20]. Davidson, D. F. and Hanson, R. K., *Int. J. Chem. Kinet.* 36(9):510-523 (2004).

2,4,4–trimethyl–1–pentene	O_2	P_5 (atm)	ϕ
0.75 %	9.0 %	1.0	1.0
0.375 %	9.0 %	1.0	0.5
0.75 %	9.0 %	4.0	1.0
0.75 %	18.0%	4.0	0.5
0.375 %	18.0%	4.0	0.25

Table 1: Experimental conditions examined for 2,4,4-trimethyl-1-pentene. The balance is argon.

Fig. 1: Retroene reaction of the 1-pentene isomer.

Fig. 2: Experimental (points) and model-predicted (lines) ignition delay times for 2,4,4-trimethyl-1-pentene oxidation behind reflected shock waves at 1.0 atm in Ar, ■ 0.75% fuel , ϕ = 1.0, ○ 0.375% fuel, ϕ = 0.5. Dashed line corresponds to open symbols. 10% error bars on experimental data.

Fig. 3: Experimental (points) and model-predicted (lines) ignition delay times for 2,4,4-trimethyl-1-pentene oxidation behind reflected shock waves at 4.0 atm in Ar, ■ 0.75% fuel, 9.0% oxygen, ϕ = 1.0, ○ 0.75% fuel, 18.0 % oxygen, ϕ = 0.5, ▲ 0.375% fuel, 18.0 % oxygen, ϕ = 0.25. Dashed line corresponds to open symbols. 10% error bars on experimental data.

Fig. 4: Experimental (points) and model-predicted (lines) ignition delay times for 2,4,4-trimethyl-1-pentene oxidation behind reflected shock waves at 0.75% fuel, ϕ = 1.0 in Ar, ■ 1.0 atm , ○ 4.0 atm. Dashed line corresponds to open symbols. 10% error bars on experimental data.

Fig. 5: Experimental (points) and model predicted (lines) ignition delay times for 0.75% fuel oxidation behind reflected shock waves at ϕ = 0.5, 4.0 atm in Ar, ■ — 2,4,4-trimethyl-1-pentene, ○ - - - 2,4,4-trimethyl-1-pentene : 2,4,4-trimethyl-2-pentene (3:1), ▲····· 2,4,4-trimethyl-2-pentene. 10% error bars on experimental data.

Fig. 6: Experimental (points) and model-predicted (line) ignition delay times for 2,4,4-trimethyl-21-pentene oxidation behind reflected shock waves at 4.0 atm in Ar, 0.75% fuel, 18.0 % oxygen, ϕ = 0.5. 10% error bars on experimental data.

Fig. 7: Sensitivity analysis showing effect of increasing rate constants by a factor of two on ignition delay time for 2,4,4-trimethyl-1-pentene. 4.0 atm, ϕ = 0.5 and T = 1242 & 1444 K.

Fig. 8: Sensitivity analysis showing effect of increasing rate constants by a factor of two on ignition delay time for 2,4,4-trimethyl-2-pentene. 4.0 atm, ϕ = 0.5 and T = 1242 & 1444 K.

Fig. 9: Decomposition of 2,4,4-trimethyl-2-pentene at 4.0 atm, ϕ = 0.5 and T = 1214 K. 10 % fuel consumed.

Fig. 10: Structures of two radicals involved in 2,4,4-trimethyl-2-pentene decomposition

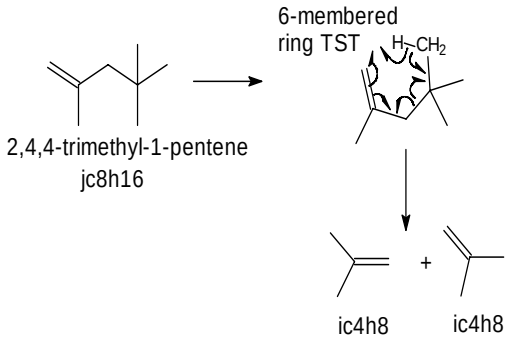

Fig. 1

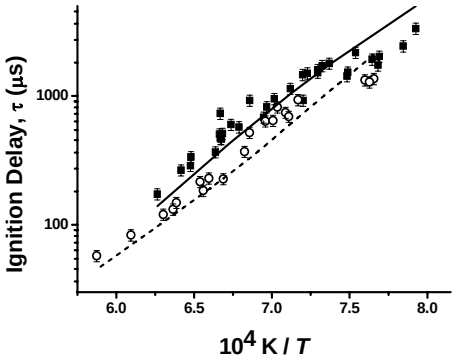

Fig. 2

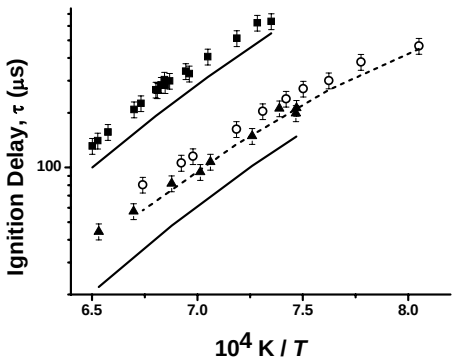

Fig. 3:

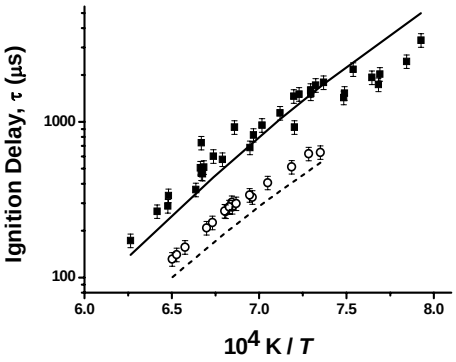
Ignition Delay, τ (μs)
1000
100
6.0
6.5
7.0
7.5
8.0
10^4 K / T

Fig. 4

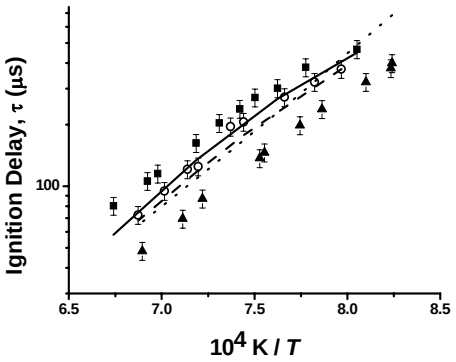
Ignition Delay, τ (μs)
100
6.5
7.0
7.5
8.0
8.5
10^4 K / T

Fig. 5

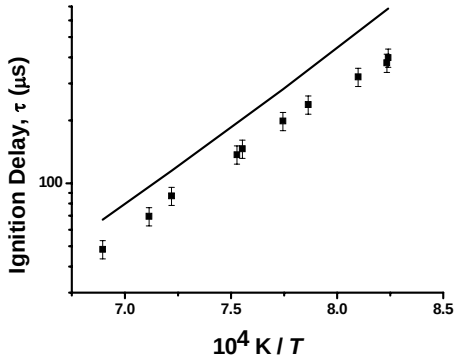

Fig. 6

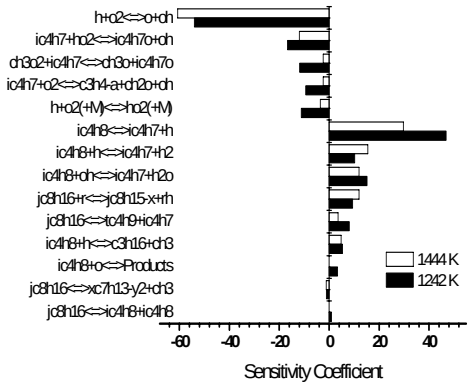

Fig. 7

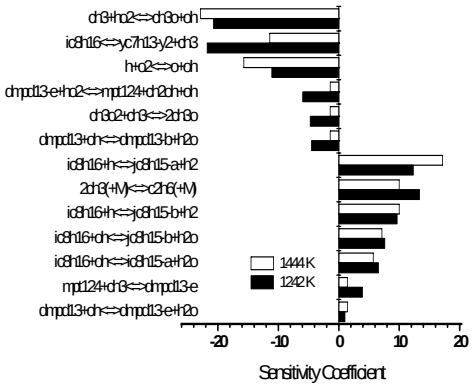

Fig. 8

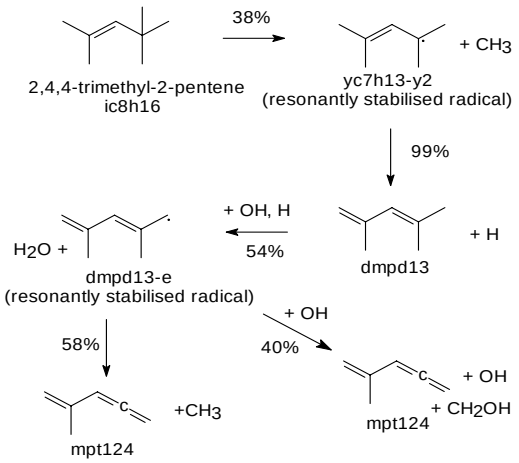
38%
+ CH3
2,4,4-trimethyl-2-pentene
ic8h16
yc7h13-y2
(resonantly stabilised radical)
99%
+ OH, H
54%
+ H
H2O +
dmpd13-e
(resonantly stabilised radical)
dmpd13
+ OH
40%
58%
+ OH
+ CH2OH
+CH3
mpt124
mpt124

Fig. 9

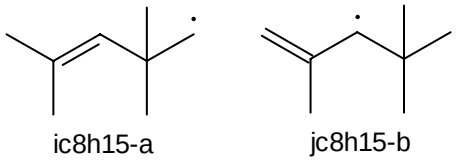
ic8h15-a
jc8h15-b

Fig. 10